 Human Molecular Genetics, 2000, Vol. 9, No. 4 503–513

ARTICLE

Long glutamine tracts cause nuclear localization of a novel form of huntingtin in medium spiny striatal neurons in *Hdh*^{Q92} and *Hdh*^{Q111} knock-in mice

Vanessa C. Wheeler[1], Jacqueline K. White[1,+], Claire-Anne Gutekunst[2], Vladimir Vrbanac[1], Meredith Weaver[1], Xiao-Jiang Li[3], Shi-Hua Li[3], Hong Yi[2], Jean-Paul Vonsattel[4], James F. Gusella[1], Steven Hersch[2], Wojtek Auerbach[5], Alexandra L. Joyner[5,6] and Marcy E. MacDonald[1,§]

[1]Molecular Neurogenetics Unit, [4]Laboratory for Molecular Neuropathology Massachusetts General Hospital, Charlestown, MA 02129, USA, [2]Department of Neurology, [3]Department of Genetics and Molecular Medicine, Emory University School of Medicine, Atlanta, GA 30322, USA, [5]Howard Hughes Medical Institute and Skirball Institute for Biomolecular Medicine and [6]Department of Cell Biology, New York University School of Medicine, New York, NY 10016, USA

Received 26 November 1999; Revised and Accepted 7 January 2000

Huntington's disease (HD) is caused by an expanded N-terminal glutamine tract that endows huntingtin with a striatal-selective structural property ultimately toxic to medium spiny neurons. In precise genetic models of juvenile HD, *Hdh*^{Q92} and *Hdh*^{Q111} knock-in mice, long polyglutamine segments change huntingtin's physical properties, producing HD-like *in vivo* correlates in the striatum, including nuclear localization of a version of the full-length protein predominant in medium spiny neurons, and subsequent formation of N-terminal inclusions and insoluble aggregate. These changes show glutamine length dependence and dominant inheritance with recruitment of wild-type protein, critical features of the altered HD property that strongly implicate them in the HD disease process and that suggest alternative pathogenic scenarios: the effect of the glutamine tract may act by altering interaction with a critical cellular constituent or by depleting a form of huntingtin essential to medium spiny striatal neurons.

INTRODUCTION

Huntington's disease (HD), with its hallmark choreiform movements and selective loss of neurons in the striatum (1,2), is caused by a dominantly inherited expanded CAG repeat that extends an N-terminal polyglutamine segment in huntingtin, an ~350 kDa protein of unknown function (3). Above ~39 glutamines (4,5), disease severity increases with glutamine number, although most HD occurs in mid-life due to polyglutamine segments of ~50 residues whereas stretches >57–60 glutamines trigger symptoms in childhood (3). The underlying process acts in a dominant fashion, causing similar disease in heterozygotes and homozygotes (6,7). It also displays selectivity for medium sized spiny neurons in the striatum due to some feature of huntingtin, as expanded glutamine tracts in unrelated proteins in each case target distinct neuronal populations causing at least seven other inherited 'polyglutamine' disorders (8–10).

The HD pathogenic mechanism, therefore, appears to comprise an attribute of huntingtin that exposes medium spiny neurons to an ultimately toxic property conferred by the polyglutamine segment. This entails a novel conformation of the N-terminus, evident in decreased electrophoretic mobility (11) and enhanced reactivity with glutamine-specific antibody reagents (12,13), although the change does not alter the stability of the protein in HD lymphoblastoid cells (14) or impair huntingtin's critical developmental activities (15). An aggregation-promoting feature of polyglutamine is implicated by its ability to drive N-terminal fragments into SDS-insoluble aggregate *in vitro* (16) with glutamine-length dependence identical to the HD mechanism (17,18). Moreover, the intimate involvement of aggregation in the disease process is revealed by nuclear N-terminal inclusions (19–22) and Congo red-staining amyloid aggregate (17), generated from full-length protein, that are found in HD post-mortem brain, although the role of aggregate *per se* is unclear (23).

What is not yet evident, in addition to the puzzling striatal specificity, is whether the pathogenic property acts at the level of the full-length mutant protein or only after its truncation (24–27). These alternative scenarios predict distinct consequences for the

[+]Present address: Department of Medicine, Wellcome Trust Addenbrooke's Hospital Site, Cambridge CB2 2XY, UK
[§]To whom correspondence should be addressed. Tel: +1 617 726 5089; Fax: +1 617 726 5735; Email: macdonam@helix.mgh.harvard.edu

context-dependent aggregation property, involving either soluble or insoluble structures for the polyglutamine segment as demonstrated in cell culture assays (13). Consequently, we are studying the *in vivo* properties of the mutant protein in *Hdh* knock-in mice, precise genetic models of adult and juvenile HD with expanded CAG repeats inserted into the murine *HD* gene (15,28). We have shown previously that accurate expression of 50-glutamine huntingtin in Hdh^{Q50} mice does not rapidly provoke abnormalities, suggesting that the mouse's short life span precludes the slow cumulative pathology of adult-onset HD (15). Therefore, we have now explored, in the striatum of Hdh^{Q92} and Hdh^{Q111} knock-in mice, the attributes conferred on huntingtin by extreme HD polyglutamine segments (92 and 111 residues) that cause symptoms in children. Our findings reveal a progressive nuclear phenotype with specificity for striatal neurons that is implicated early in the disease process in man by critical features shared with the HD pathogenic property.

RESULTS

Altered structure of accurately expressed huntingtin in Hdh^{Q92} and Hdh^{Q111} mice

In typical HD heterozygotes, mutant and normal huntingtin are both expressed in an apparently similar fashion (6,7). Therefore, we examined the expression of mutant huntingtin with 92 or 111 glutamines, encoded by the CAG expansion allele, and the 7-glutamine wild-type protein, produced from the Hdh^{+} allele, in the cells and tissues of heterozygous Hdh^{Q92}/Hdh^{+} and Hdh^{Q111}/Hdh^{+} knock-in mice. The results of immunoblot analysis of proteins precipitated from extracts of Hdh^{Q92}/Hdh^{+} brain and peripheral tissue by HF1, an antibody to internal epitopes (14), are shown in Figure 1A, and reveal appropriate expression of mutant and wild-type huntingtin. Probing with huntingtin mAb 2166 reveals a band of mutant protein (>340 kDa) that mirrors the wild-type huntingtin band (~340 kDa) in all tissues surveyed (brain, testis, spleen, liver, lung), although its long polyglutamine segment causes decreased mobility.

Immunoblot experiments with Hdh^{Q50}, Hdh^{Q92} and Hdh^{Q111} brain extracts (Fig. 1B) demonstrate the HD-like altered structural properties conferred by polyglutamine segments ranging from 50 to ~111 residues. In each case, HF1 detects a band of mutant protein that migrates progressively higher in the gel compared with the wild-type protein in the heterozygote, whereas homozygous littermates express two copies' worth of mutant protein. Probing with mAb 1F8, specific for long soluble glutamine (13,17), does not detect the short polyglutamine segment in the wild-type protein, but reveals the mutant band with a signal intensity that increases with expanded glutamine number. Notably, we do not observe additional genotype-specific bands in these experiments, suggesting that the stability of the bulk of the mutant protein is not altered compared with wild-type.

Glutamine-dependent mutant huntingtin in the nucleus of striatal neurons

We then investigated whether the polyglutamine segments confer altered properties in striatal neurons *in vivo* by immunostaining sections of young homozygote striatum with N-terminal huntingtin antibody, EM48 (21). Typical micrographs (Fig. 2) document a remarkable change in the subcellular location of EM48 reactivity. At the youngest age (1.5 months) EM48 reactivity is found in the cytoplasm of abundant striatal neurons in both lines of mice, although notable clusters of Hdh^{Q111}/Hdh^{Q111} cells in the ventral region exhibit weak 'equal' staining of both cytoplasm and nucleus whereas a few neurons display faint nuclear reactivity without cytoplasmic EM48 stain. This pattern is also found in Hdh^{Q92}/Hdh^{Q92} striatum but at an older age (2.5 months) when the majority of EM48-reactive Hdh^{Q111}/Hdh^{Q111} neurons exhibit prominent nuclear signal. Later, at 4.5 months, EM48 reactivity is confined to the nucleus of many striatal neurons in homozygotes of both lines, although the signal for the 111-glutamine protein is more punctate. However, this striking age and glutamine-dependent 'relocation' of EM48 reactivity to the nucleus is not associated with rapid neuronal cell dysfunction, as Hdh^{Q92} and Hdh^{Q111} knock-in mice do not differ from wild-type littermates in routine behaviors or in their performance in quantitative tests (data not shown).

A distinct form of huntingtin relocalizes to the nucleus in mutant striatum

To identify which striatal neurons support the 'redistribution' of EM48 reactivity, we assessed homozygous mutant striatum by double-label microscopy using EM48 and markers of different neuronal classes. As shown for homozygous mutant striatum in Figure 3A, EM48 does not stain vesicular acetylcholine transporter (VAT), NOSI or parvalbumin-reactive cells but rather detects the nuclei of calbindin-D-positive cells, indicating a process detected by EM48 that occurs in medium sized spiny neurons targeted in HD. To determine whether nuclear staining is detected by internal huntingtin reagents we double-stained sections with HF1 and calbindin-D (Fig. 3A). In this case, however, we observed punctate signal in the neuropil and the cytoplasm of both calbindin-D-positive and -negative neurons, an often-reported pattern that reflects the broad huntingtin mRNA distribution (29–32), but which is distinct from that of EM48. Thus, as is evident from a comparison of the micrographs in Figure 3A, nuclear EM48 reactivity is not coincident with the HF1 signal, but rather is found only in the calbindin-D-positive subset of HF1-stained neurons. Although other scenarios are possible, this suggests that medium spiny neurons display distinct forms of the mutant protein with a form particularly reactive for EM48 located in the nucleus.

We then examined striatum from wild-type littermates in the same manner and, as shown in Figure 3B, discovered the same discordant EM48 and HF1 staining patterns that were observed in mutant neurons, except that EM48 reactivity is confined to the cytoplasm of calbindin-D-positive cells. Thus, in wild-type striatum EM48 also detects only a subset of those neurons stained by HF1, suggesting that these medium spiny neurons, in contrast to most other cells, possess alternate forms of huntingtin distinguished by the accessibility of N-terminal EM48 epitopes. In our immunoblot experiments we do not observe striatal-specific truncated huntingtin fragments that would indicate alternate cleaved N- and C-terminal products. The immunostaining results, therefore, are more consistent with a property of medium spiny neurons that promotes the participation of full-length huntingtin in a conformation or in complexes that 'expose' the N-terminus. In this scenario, the N-terminal accessible version of the protein appears to be redistributed to the nucleus in mutant spiny neurons,

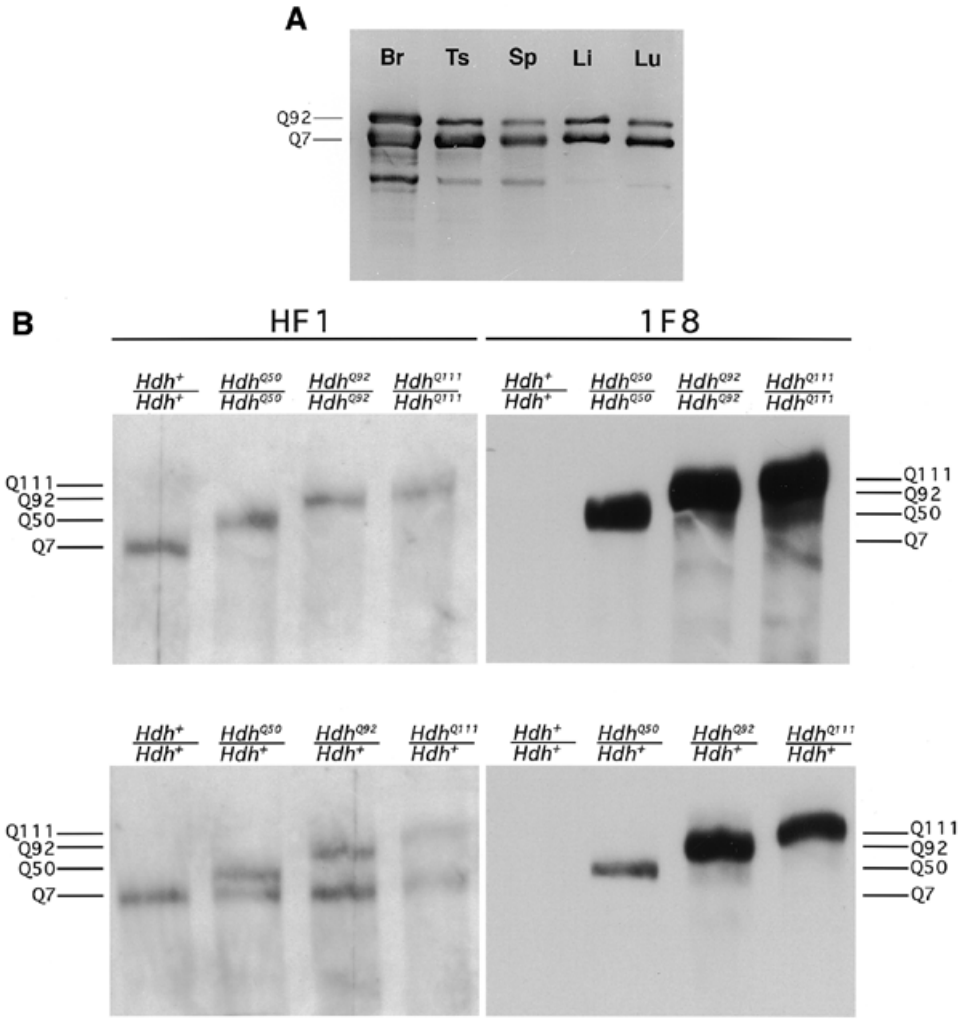

Figure 1. Accurate expression of mutant huntingtin with altered structural properties. (**A**) Mutant and wild-type proteins display identical expression patterns. An immunoblot, detected by mAb 2166, of HF1-immunoprecipitated proteins from Hdh^{Q92}/Hdh^{Q+} heterozygote brain (Br), testis (Ts), spleen (Sp), liver (Li) and lung (Lu) is shown. Mutant (Q92) and wild-type (Q7) (~340 kDa) huntingtin are indicated. Lower molecular weight bands are variable degradation products arising during the experiment. Decreased intensity of the mutant compared with the wild-type band is typical and in HD lymphoblasts is not associated with altered instability of the mutant protein (14). (**B**) Altered properties of mutant compared with wild-type huntingtin. An immunoblot, detected with HF1, of brain proteins from wild-type (Hdh^{+}/Hdh^{+}) littermate or homozygous (top) and heterozygous (bottom) Hdh^{Q50}, Hdh^{Q92} and Hdh^{Q111} mice. Mutant (Q50, Q92, Q111) bands (>340 kDa) and the wild-type (Q7) band (~340 kDa) are indicated. The same immunoblot probed with mAb 1F8 reveals only the mutant protein with its elongated polyglutamine tracts. Equal amounts of protein are loaded in each lane.

whereas the form that is not detected by EM48 remains in the cytoplasm.

Nuclear localization appears to involve full-length mutant protein

To directly test the alternative explanations and to identify huntingtin in the nucleus of mutant striatal neurons, we compared proteins extracted from subcellular fractions prepared from Hdh^{Q92}/Hdh^{Q92} striatum and cortex. At 7.5 months of age all neurons in the striatum display cytoplasmic HF1 reactivity and ~80% also exhibit a nuclear EM48 signal. In contrast, although the majority of cells in the cerebral cortex also possess an HF1 signal in the cytoplasm, <5% display EM48 reactivity, and this too is cytoplasmic. When immunoblots of nuclear and cytosolic proteins, displayed on SDS–PAGE, are detected with N-terminal and internal huntingtin antibodies (Fig. 4) the only EM48-reactive protein enriched in the striatal nuclear fraction is a band of full-length mutant huntingtin that is also detected by 1F8 but not HF1, a less sensitive reagent in this format. In comparison, a very faint 1F8 reactive band of full-length protein is found in the cortical nuclear fraction but this is not detected with either EM48 or HF1. All three reagents each detect a different set of bands, especially in the low molecular weight range. However, none of these is specific to either the nuclear or the cytosolic fraction from striatum, precluding striatal-specific truncated N- or C-terminal fragments that could explain discordant EM48 and HF1-staining patterns. On the other hand, the weak band of full-length protein in the nuclear fraction of striatal neurons suggests that a small proportion of the >350 kDa mutant protein may be involved in nuclear 'relocation' of EM48 epitopes.

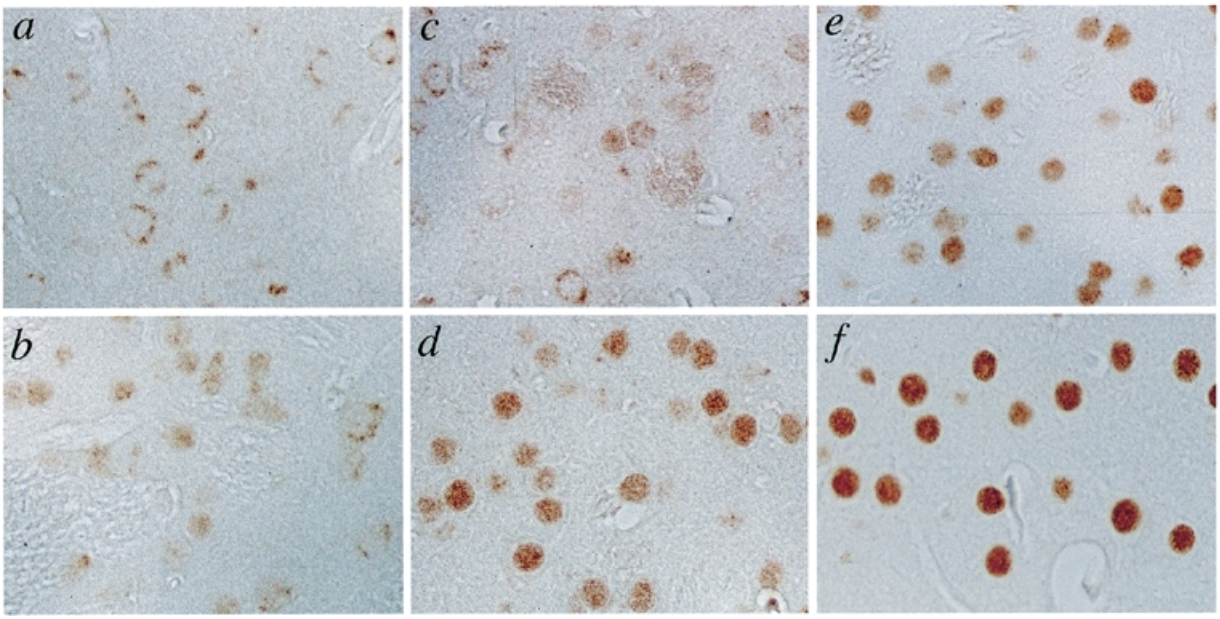

Figure 2. Age- and polyglutamine size-dependent nuclear 'relocation' of EM48 reactivity. Light micrographs of EM48 immunostaining of striatum are shown. (**a**) Cytoplasmic staining of Hdh^{Q92}/Hdh^{Q92} neurons at 1.5 months. (**b**) Neurons exhibiting both weak nuclear and cytoplasmic reactivity in Hdh^{Q111}/Hdh^{Q111} ventral striatum at 1.5 months and (**c**) in Hdh^{Q92}/Hdh^{Q92} at 2.5 months. Neurons display exclusively nuclear staining in Hdh^{Q111}/Hdh^{Q111} at 2.5 months (**d**), and at 4.5–5 months for Hdh^{Q92}/Hdh^{Q92} (**e**) and Hdh^{Q111}/Hdh^{Q111} (**f**) homozygotes.

Nuclear but not cytoplasmic EM48 staining of heterozygous neurons

The pathogenic property conferred on the mutant protein in HD is dominantly inherited, prompting us to test both whether nuclear EM48 redistribution occurs in heterozygous *Hdh* knock-in mice and, if it does, whether it occurs with the same properties as those that we observe in homozygous littermates. We therefore compared the EM48 staining patterns in striatum of Hdh^{Q111}/Hdh^{+} heterozygotes and Hdh^{Q111}/Hdh^{Q111} homozygotes at ages when in the latter extensive nuclear EM48 reactivity is observed (2.5 months) and later when all medium spiny neurons are involved (5 months). As demonstrated by the micrographs in Figure 5, at the younger age, prominent nuclear EM48 reactivity is observed in the striatum of the homozygote but most EM48-positive neurons in the heterozygous littermate display cytoplasmic reactivity. By 5 months of age, however, the EM48 signal is confined to the nucleus in the heterozygote as well as the homozygote, demonstrating that nuclear localization occurs in the presence of the wild-type protein. Moreover, the lack of cytoplasmic staining in the heterozygous neurons reveals that the process triggered by the mutant protein can recruit wild-type EM48-reactive protein to the nucleus, although doubling the dose of mutant protein may subtly affect the timing of nuclear 'relocation'.

Nuclear phenotype is progressive and entails formation of morphologic inclusions

Our assessment of older Hdh^{Q92} and Hdh^{Q111} mice (Fig. 6A, and summarized for all ages in Fig. 6B) demonstrates that the EM48 nuclear phenotype is progressive. In striatum at ages ranging from 10–15 months of age, strong diffuse EM48 reactivity is overlaid either with darkly reactive puncta or, at the oldest ages, with a single dot. These dots are also detected with antibodies to ubiquitin, suggesting that these entities are similar to nuclear inclusions (data not shown). However, reactivity for internal huntingtin epitopes, including mAb HD549, is found only in the neuropil and neuronal cytoplasm confirming that the bulk of huntingtin does not participate in the nuclear phenotype. Thus, EM48-reactive inclusions form ~9–10 months after diffuse nuclear staining is apparent, indicating that the precipitating event occurs late in the phenotype.

When the patterns of EM48 reactivity at all ages are compared (Fig. 6B) it is evident that the longer of the two expanded polyglutamine segments provokes a more rapid phenotype. For example, inclusions are apparent at ~10 months with 111 glutamines, whereas these occur at ~12–15 months with 92 residues. It is also noteworthy that this progressive glutamine-dependent process, which involves the major population of neurons in the striatum, also occurs in a minor proportion of cells in other brain regions in a gradient from youngest to oldest (1.5–10 months): striatum > olfactory tubercle >> pyriform cortex = cerebral cortex. Indeed, in older mice a few EM48-reactive nuclei are found in septum, olfactory bulb, nucleus accumbens, cerebellar granule cell layer and hippocampus. However, despite this striking and progressive EM48-nuclear phenotype we do not find evidence of overt neuronal cell death, neuronal dysfunction (quantitative gait and rotarod analyses) or overt pathology, although a subtle reduction in nuclear volume may suggest shrinkage of neurons in the striatum (data not shown).

Insoluble aggregate concomitant with the inclusion stage

The structural property conferred by polyglutamine expansion generates amyloid aggregate from full-length protein in HD post-mortem brain. We therefore assessed the involvement of insoluble polyglutamine in the EM48-nuclear phenotype using filter trap

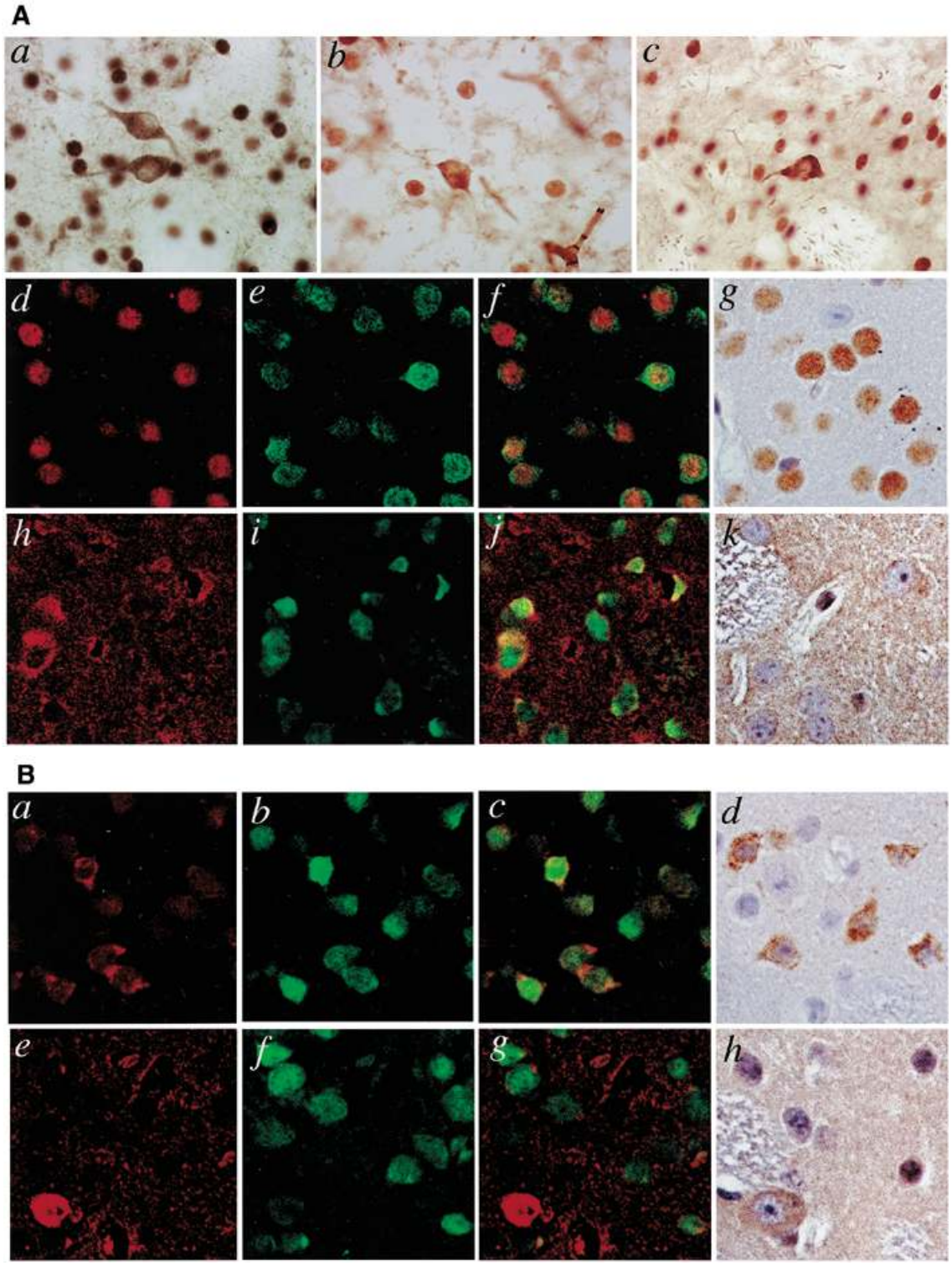

Figure 3. EM48 reactivity in a subset of HF1-positive striatal neurons. (**A**) Mutant striatum: nuclear EM48 reactivity in the calbindin-D-positive subset of HF1-reactive neurons. Typical light microscope (a–c, g, k) and confocal (d–f, h-j) images of Hdh^{Q92}/Hdh^{Q92} (a–c) and Hdh^{Q111}/Hdh^{Q111} (d–k) striatum stained with either EM48 (a–g) or HF1 (h–k). Double labeling reveals no EM48-reactive nuclei in interneurons (a–c) identified by cytoplasmic VAT (a), NOSI (b) or parvalbumin (c) staining. EM48-reactive nuclei (red) (d) are detected in calbindin-D-positive (green) medium spiny neurons (e). (f) Overlapped image. HF1-reactive neuropil and cytoplasm (red) (h) of neurons that comprise calbindin-D-positive (green) and -negative cells (i). (j) Overlapped image. (g and k) Sections are counterstained with hematoxylin. (a–c) Neurons at 12 and (d–k) at 5 months. (**B**) Wild-type striatum: cytoplasmic EM48 reactivity in the calbindin-D-positive subset of HF1 reactive neurons. Confocal (a–c, e–g) and light microscope (d and h) images of wild-type littermate striatum stained with EM48 (a–d) or HF1 (e–h). Double labeling reveals cytoplasmic EM48 reactivity (red) (a) in calbindin-D-positive (green) medium spiny neurons (b). (c) Overlapped image. HF1-reactive neuropil and cytoplasm (red) (e) of neurons that comprise calbindin-D-positive (green) and -negative cells (f). (g) Overlapped image. (d–h) Sections are counterstained with hematoxylin. (a–h) Neurons at 5 months.

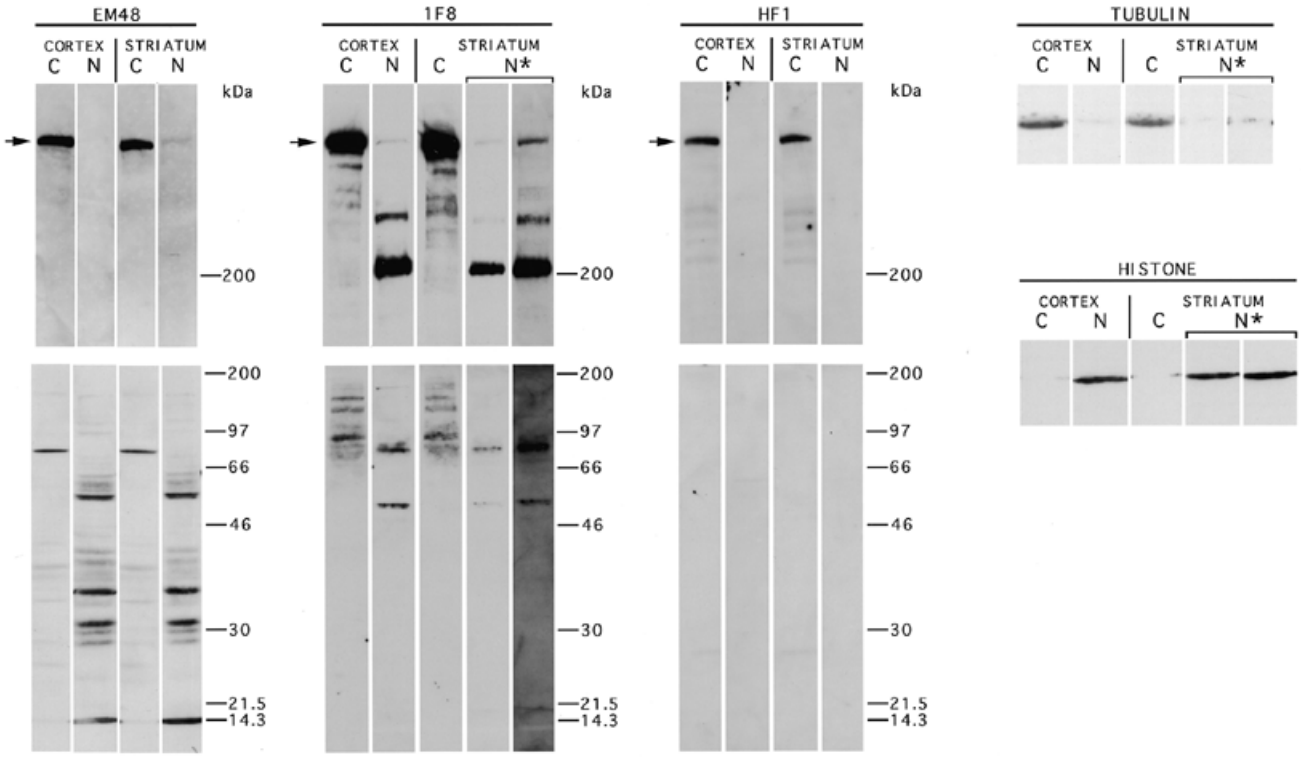

Figure 4. Nuclear 'redistribution' of EM48 reactivity involves full-length mutant protein. Immunblots of proteins extracted from subcellular cytosolic (C) and nuclear (N) fractions of Hdh^{Q92}/Hdh^{Q92} striatum and cortex probed with EM48, mAb 1F8 and HF1 are shown. (Top) ~200–340 kDa range. (Bottom) 14–200 kDa range. The full-length mutant huntingtin band is indicated by an arrow. Note: each lane contains ~160 µg of protein, except the striatal nuclear fraction where the entire 30 µg yield was loaded. For this fraction, a longer exposure (*) of 1F8 is provided. Longer exposures of HF1 and EM48 detected blots did not reveal additional bands (data not shown). The 1F8 signal in (*) ~21.5 kDa marker is a staining artifact. To assess purity of the cytosolic and nuclear fractions the membranes were probed with α-tubulin and histone H2B, respectively. A longer exposure (*) for the striatal nuclear fraction is provided.

assays to monitor insoluble aggregate in SDS-enriched nuclear fractions from striatum (at ages typifying each morphologic stage) of Hdh^{Q92} and Hdh^{Q111} homozygotes, their wild-type littermates and post-mortem HD and control brain. The results of probing the filter-immobilized fractions with EM48, 1F8 and HF1 are presented in Figure 7 and clearly demonstrate EM48-reactive aggregate only in fractions from HD brain and older mouse mutants (10–14.5 months). All EM48-reactive fractions are 1F8 negative, confirming the insolubility of the glutamine tract in these complexes. These also are not detected by HF1, implying truncated protein as suggested for Congo red-positive insoluble aggregate from HD post-mortem brain (17). The timing of insoluble aggregate does not correlate with diffuse EM48 reactivity, but rather with the appearance of morphologic inclusions, suggesting a relationship between the two. In any case, the event that triggers the formation of insoluble aggregate occurs late in the nuclear phenotype, precluding its involvement in the mechanism that initiates nuclear EM48 'redistribution'.

DISCUSSION

In HD the structural property conferred on the mutant protein comprises a feature of huntingtin that determines striatal specificity and an ultimately toxic attribute of polyglutamine (8,33). Although the accumulated evidence points to the promotion of aggregation, it is not clear whether this property triggers pathogenesis in the context of full-length protein or a truncated product (24–27), and in either scenario the specificity for striatal neurons is unexplained. Our studies in precise knock-in mouse models of juvenile HD reveal that extreme HD polyglutamine segments alter mouse huntingtin, changing its mobility and reactivity with 1F8, without altering the stability of the bulk of the protein, consequences first observed in the cells and tissues of HD patients (11,12).

In addition, we have identified *in vivo* correlates in striatal neurons, including the 'relocation' of mutant protein to the nucleus in medium sized spiny neurons, cells that are primary targets in HD, and much later the formation of morphologic nuclear inclusions and insoluble aggregate reported in post-mortem HD brain (17–22). The underlying property shares critical features of the HD-specific mechanism: sensitivity to polyglutamine size and dominance, with heterozygotes and homozygotes exhibiting a similar phenotype, although the mouse's short life span precludes comparison of glutamine thresholds and may limit the ultimate toxic consequences. This cohort of shared attributes provides strong evidence that the novel property conferred by long polyglutamine segments in *Hdh* knock-in striatal neurons is the same feature that triggers pathology and aggregate formation in HD. Thus, nuclear 'relocation' of mutant protein and subsequent formation of aggregate are likely to be early linked events in the disease process in man.

In HD the altered N-terminal conformation could act within the full-length protein or perhaps must first be cleaved to release a

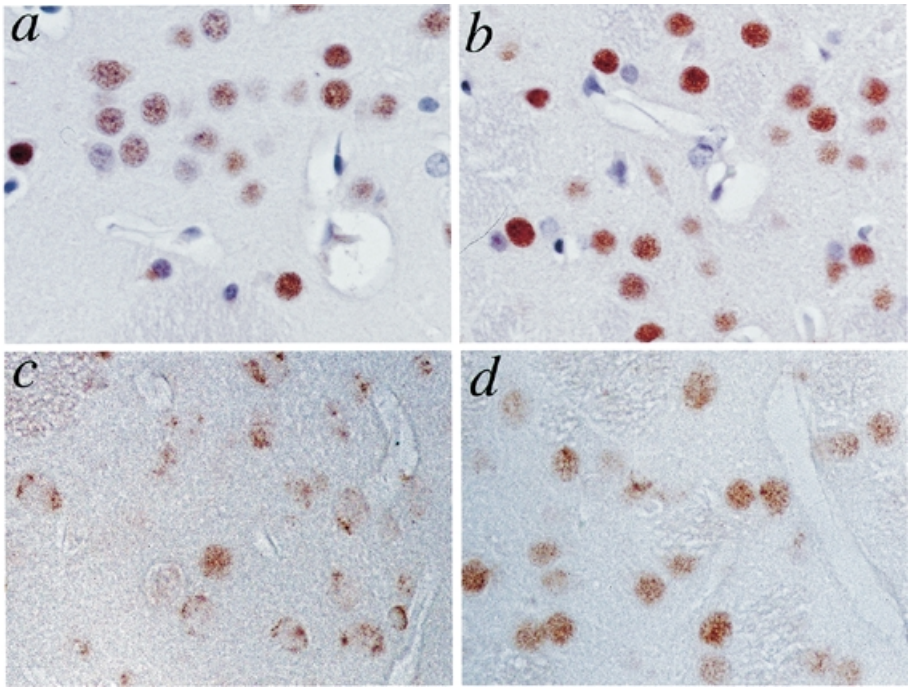

Figure 5. Nuclear 'relocation' of EM48 reactivity is dominant and recruits wild-type protein. Light micrographs of EM48 immunostaining of striatum. Hdh^{Q111}/Hdh^{Q+} heterozygote at 5 months (**a**) and 2.5 months (**c**), and Hdh^{Q111}/Hdh^{Q111} homozygote at 5 months (**b**) and 2.5 months (**d**). The similarity of the staining patterns in (a) and (b) indicates a dominantly inherited redistribution of reactivity that in the heterozygote also 'relocates' the wild-type signal, which in wild-type neurons is invariably cytoplasmic. (a and b) Sections are counterstained with hematoxylin.

'toxic' fragment (24–27) in some manner that explains the selectivity for medium spiny striatal neurons. The earliest step in the *Hdh* knock-in nuclear phenotype that we can discern, nuclear EM48 staining, does not involve truncated fragment with soluble or insoluble polyglutamine as demonstrated by results of immunoblot, immunoprecipitation and filter-trap experiments. Enrichment of a band of full-length mutant protein in nuclear proteins from striatal cells, however, is consistent with the participation of the entire protein. This possibility also resolves the conundrum posed by discordant neuronal distributions of EM48 and internal huntingtin epitopes that we also observe, in the absence of culpable truncated fragment on immunoblots, in wild-type striatum. Our data, therefore, support a scenario in which medium spiny neurons can promote the formation of a distinct version of full-length huntingtin with an accessible N-terminus, rather than stable cleaved N- and C-terminal products as previously proposed (27).

In this scenario, mutant huntingtin shares with the wild-type protein the ability to assume a discrete conformation or to participate in complexes that 'expose' the N-terminus, 'presenting' the polyglutamine segment to medium spiny neurons in a fashion that triggers nuclear 'relocation' of EM48 reactivity in *Hdh* knock-in mice. It is likely that this feature of huntingtin accounts for the specificity of the closely related pathogenic property in HD, implicating a soluble polyglutamine segment in the context of full-length huntingtin in triggering the cascade of events that culminates in HD pathology.

The consequences of progressive nuclear 'relocation' and subsequent formation of morphologic dots, resembling inclusions, and insoluble aggregate appear to be subtle, causing no rapid overt neuronal dysfunction in Hdh^{Q92} and Hdh^{Q111} mice but rather may be associated with decreased nuclear volume of striatal neurons, suggesting cell shrinkage. The abnormal N-terminal nuclear deposits, and insoluble aggregate, therefore, are not sufficient to trigger immediate cell death or neuronal dysfunction (24,34), although the long-term cumulative effects of the property that propels their formation may ultimately produce neuronal toxicity. Importantly, the finding that accurately expressed mutant huntingtin with extreme HD glutamine tracts causes onset of overt dysfunction in childhood in man but not in mice supports a disease process that operates in a time-dependent rather than a developmental stage-dependent manner. This is consistent with the insidious progressive nature of HD pathology in man, which appears to begin from birth (35), and with the absence of dramatic phenotypes in a similar *Hdh* knock-in line (36). In contrast, several transgenic HD mouse models exhibit a variety of dramatic phenotypes, including overt cell death (27,37), neuronal dysfunction (27,34,37,38) and shortened life span (34,37,38). These phenotypes are due to distinct molecular contexts of the long polyglutamine segment, including over-expression, inappropriate structure (truncations) and alteration of the genetic background due to insertion and coincident expression of additional genes (e.g. YACs). Thus, the artificial nature of the transgenes together with the subtlety of the phenotype associated with appropriate expression of mutant huntingtin in precise genetic models, *Hdh* knock-in lines, suggests that the dramatic HD transgenic phenotypes may not be due exclusively to the pathogenic process that operates in the human disease. It is difficult to predict whether Hdh^{Q92} and Hdh^{Q111} mice will develop phenotypes that are similar to transgenic models or will reveal additional novel phenotypes. Indeed, our discovery of a property that provokes nuclear redistribution of a form of mutant protein in medium spiny neurons that has the capacity to relocate the wild-type version suggests alternative gain-of-function scenarios for HD pathogenesis. The altered structure imposed on the 'exposed' N-terminus by an elongated polyglutamine stretch may involve

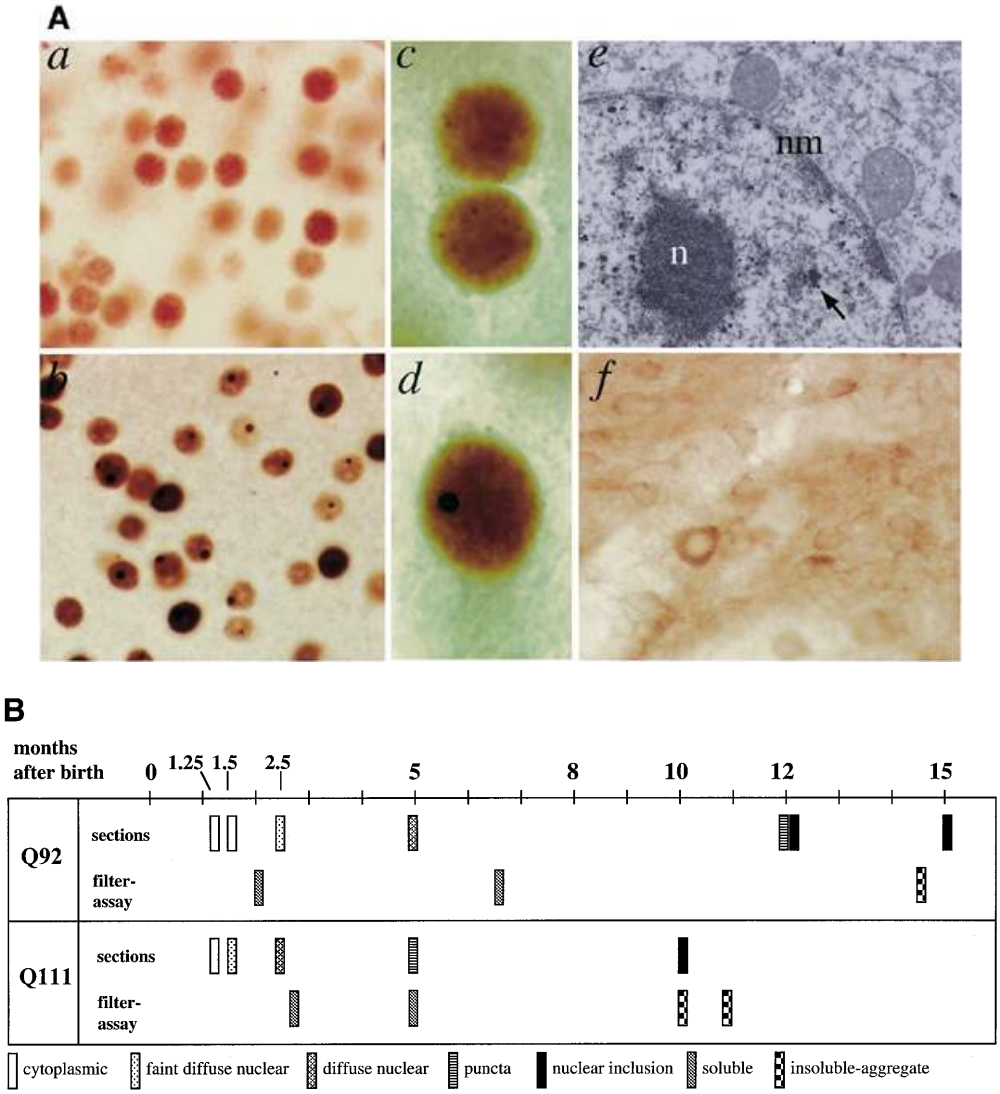

Figure 6. The nuclear phenotype is progressive and entails the late formation of inclusions. (**A**) Formation of EM48-reactive nuclear inclusions at older ages in Hdh^{Q92}/Hdh^{Q92} striatum. Light (a–d and f) and electron (e) micrographs of EM48 immunostaining. Diffuse nuclear reactivity, overlaid with disperse puncta at 12 months (a, c and e). (e) Arrow denotes small nuclear immunogold clusters that are likely to correspond to puncta observed by light microscopy. n, nucleolus; nm, nuclear membrane. (b and d) A single nuclear inclusion augments diffuse and punctate staining at 15 months. (f) mAb HD549 detects only cytoplasmic and neuropil staining. (**B**) Nuclear striatal phenotype is progressive and glutamine dependent. Stages of the EM48-reactive nuclear phenotype in Hdh^{Q92}/Hdh^{Q92} (Q92) and Hdh^{Q111}/Hdh^{Q111} (Q111) striata as monitored by immunohistochemistry and filter-trap assay of SDS-insoluble protein fractions. Immunohistochemical staining patterns are defined as cytoplasmic (unfilled), faint diffuse nuclear (speckled), diffuse nuclear (hatched), puncta (striped) and nuclear inclusion (black). Filter assay results are designated EM48-negative, soluble (grey) and EM48-positive, insoluble (checkered). The 5 month Q111 filter-trap result was obtained by assaying whole brain. Puncta or nuclear inclusions were detected for Q92 at 12 months ($n = 2$), whereas multiple determinations for all other age–genotype combinations yielded identical results ($n = 2$–3).

huntingtin with other critical cellular constituents or, alternatively, it may act via the gradual loss of an essential functional form of huntingtin in mature spiny striatal neurons with ultimately devastating consequences.

MATERIALS AND METHODS

Hdh^{Q50}, Hdh^{Q92} and Hdh^{Q111} knock-in mice

Hdh^{Q50}, Hdh^{Q92} and Hdh^{Q111} knock-in mice with targeted insertion of a chimeric human–mouse exon 1 with 48, 90 and 109 CAG repeats, respectively (15,28), used in this study were maintained on a mixed 129/CD1 genetic background by breeding to CD1 (Charles River Laboratories, Wilmington, MA). Genotyping by Southern blot analyses and PCR assay for CAG repeat size were performed as described (15,28). *Hdh* CAG knock-in lines are in the Induced Mutant Mouse Repository (Jackson Laboratory, Bar Harbor, ME).

Antibody reagents

Huntingtin antibody reagents were typically affinity purified: EM48 (amino acids 1–256) (21), HF1 (amino acids 1981–2580) (14), mAb HD549 (amino acids 549–679) (31), mAB2166 (amino acids 181–810) (Chemicon International, Temecula, CA) and mAb 1F8 glutamine segments >39 (14,17). Other reagents were: mAb calbindin-D (Sigma, St Louis, MO), anti-VAT (39) for cholinergic interneurons, anti-parvalbumin for medium sized

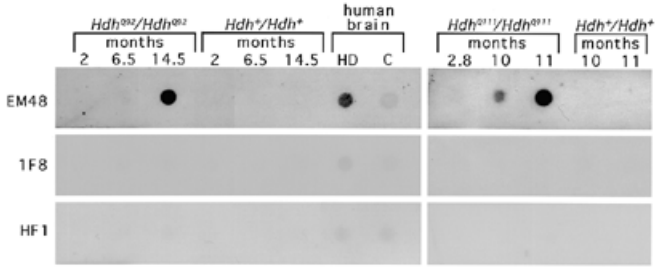

Figure 7. Detergent-resistant EM48-reactive N-terminal aggregate is a late event. Detection of membrane-trapped SDS-enriched fractions with EM48, HF1 and mAb 1F8. Detergent enriched fractions are from Hdh^{Q92}/Hdh^{Q92} and wild-type littermate striatum (2, 6.5 and 14.5 months), Hdh^{Q111}/Hdh^{Q111} and wild-type striatum (2.8, 10 and 11 months) and frontal cortex of HD and control brain.

interneurons (PARV; Sigma) and nitric oxide synthase for somatostatin and neuropeptide Y neurons (NOSI; Chemicon), anti-glial fibrillary acidic protein for reactive gliosis (GFAP; Dako, Carpinteria, CA), anti-histone H2B, ubiquitin (Chemicon) and anti-α-tubulin (Sigma).

Preparation of soluble proteins, immunoprecipitation and immunoblot analyses

Soluble proteins extracted from brain and peripheral tissues by hypotonic lysis (50 mM Tris–HCl pH 7.5, 10% glycerol, 5 mM magnesium acetate, 0.2 mM EDTA with 0.5 mM DTT, 170 µg/ml PMSF, 10 µg/ml leupeptin and 2 µg/ml aprotinin) were first immunoprecipitated or directly electrophoresed in 5% SDS–polyacrylamide gels as described (15). Fractionation of striatum and cortex was carried out at 4°C using dissected tissue pooled from six mice. Tissue was homogenized in 15 vol of homogenization buffer (0.3 M sucrose, 50 mM Tris–HCl pH 7.5, 2.5 mM magnesium acetate, 0.25% Triton X-100, containing protease inhibitors), filtered through two layers of gauze, and centrifuged at 500 *g* for 5 min. The pellet was resuspended in 2 ml 2.4 M sucrose, 50 mM Tris–HCl pH 7.5, 2.5 mM magnesium acetate, 0.1% Triton X-100 containing protease inhibitors, centrifuged at 100 000 *g* for 1 h, and the resulting nuclear pellet resuspended in homogenization buffer without Triton X-100. The supernatant from the 500 *g* spin was centrifuged at 100 000 *g* for 1 h and the supernatant kept as the cytosolic fraction. Nuclear and cytosolic fractions were electrophoresed in 12 or 5% SDS–PAGE. Proteins were transferred from PAGE by electroblot to PVDF membrane. ECL antibody detection was enhanced using an avidin–biotin complex (Vectastain ABC kit; Vector Laboratories, Burlingame, CA). Protein was quantitated using the detergent compatible Lowry assay (Bio-Rad, Hercules, CA).

Filter trap assay

SDS-insoluble protein was extracted from an ~2 mm coronal slice of mouse brain that contained striatum and from human post-mortem HD and control cortex and monitored by filter capture on cellulose acetate membrane as described previously (17).

Light and confocal microscopy and immunohistochemistry

Light microscopic immunohistochemistry was on 7 µm coronal sections of periodate-lysine-paraformaldehyde (PLP) perfused and post-fixed brain, embedded in paraffin as described (15). For detection sections were microwaved in 0.01 M sodium citrate buffer pH 6, incubated in methanol/0.3% H_2O_2 (30 min), blocked in TBS/3% normal goat serum (NGS), and incubated with primary antibody in TBS/1% NGS (16 h). TBS washed sections were incubated in TBS/1% NGS with biotinylated anti-rabbit IgG (1:200 dilution; Vectastain Elite ABC kit; Vector Laboratories) and detected using an avidin–biotin complex (Vectastain Elite) and 3,3′-diaminobenzidine (DAB) (FAST DAB peroxidase tablet set; Sigma). Some sections were counterstained with hematoxylin. For confocal microscopy the secondary antibodies were Cy3-conjugated goat anti-rabbit and Cy2-conjugated goat anti-mouse (Jackson ImmunoResearch Laboratories, West Grove, PA). Electron and light microscopic analyses of some brains (Hdh^{Q92} 12 and 15 months; Hdh^{Q111} 10 months) and double labeling (EM48 with VAT, parvalbumin, NOSI) were on 40 µm coronal sections from brains perfused with 3% paraformaldehyde, 0.15% gluteraldehyde (in 0.1 M phosphate buffer pH 7.2) and post-fixed in 1% paraformaldehyde. Toluidine blue staining on ultra-thin sections to identify pathologic changes and immunostaining were as described previously (21,31). Control sections omitted primary antibody and for double labeling adjacent sections were incubated with a single primary antibody. TUNEL staining on deparaffinized 7 µm paraffin-embedded sections was as described (40).

Routine and quantitative behavioral analyses

Hdh^{Q92} and Hdh^{Q111} and wild-type littermates (2–17 months of age) do not differ in routine behaviors (breeding, weight gain), brain to body weight ratio, life span, suspended paw clasp, exploratory behavior, response to foreign cage or intruder, or in aggressiveness, reported for another *Hdh* knock-in line (35). Resting blood glucose levels and response to glucose load do not differ with genotype, indicating that Hdh^{Q92} and Hdh^{Q111} mice do not develop diabetes as do *HD* exon 1 transgenic mice (41). Quantitative tests (42) of gait (stride length, width, consistency) or performance on accelerating rotarod (Basile Rota-rod Treadmills, Stoelting, IL) do not distinguish mutant mice and wild-type littermates.

ACKNOWLEDGEMENTS

We thank Ms W. Hobbs, J. Srinidhi, L. Lebel and C. Dorn for technical assistance, and Drs C. Huang, S. Namura, F. Persichetti, S. Browne and O. Andreasson for their expertise and discussion. We are grateful to Drs M. Schwarzschild and J.-F. Chen for generously providing rotarod apparatus and Dr E. Burright for furnishing the gait tunnel. J.K.W. was the recipient of the Lieberman Award of the Hereditary Disease Foundation. This work was supported by NINDS grants NS32765 and NS16367 and grants from the Foundation for the Care and Cure of Huntington's Disease and the Huntington's Disease Society of America (Coalition for the Cure). A.L.J. is an Investigator of the Howard Hughes Medical Institute.

REFERENCES

1. Folstein, S. (1989) *Huntington's Disease: A Disorder of Families*. Johns Hopkins Press, Baltimore, MD.
2. Vonsattel, J.P. and DiFiglia, M. (1998) Huntington disease. *J. Neuropathol. Exp. Neurol.*, **57**, 369–384.

3. Huntington's Disease Collaborative Research Group (1993) A novel gene containing a trinucleotide repeat that is expanded and unstable on Huntington's disease chromosomes. *Cell*, **72**, 971–983.
4. McNeil, S., Novelletto, A., Srinidhi, J., Barnes, G., Kornbluth, I., Altherr, M.R., Wasmuth, J.J., Gusella, J.F., MacDonald, M.E. and Myers, R.H. (1997) Reduced penetrance of the Huntington's disease mutation. *Hum. Mol. Genet.*, **6**, 775–779.
5. Rubinsztein, D.C., Leggo, J., Coles, R., Almqvist, E., Biancalana, V., Cassiman, J.J., Chotai, K., Connarty, M., Crauford, D., Curtis, A. *et al.* (1996) Phenotypic characterization of individuals with 30–40 CAG repeats in the Huntington disease (HD) gene reveals HD cases with 36 repeats and apparently normal elderly individuals with 36–39 repeats. *Am. J. Hum. Genet.*, **9**, 16–22.
6. Wexler, N.S., Young, A.B., Tanzi, R.E., Travers, H., Starosta-Rubinstein, S., Penney, J.B., Snodgrass, S.R., Shoulson, I., Gomez, F., Ramos Arroyo, M.A. *et al.* (1987) Homozygotes for Huntington's disease. *Nature*, **326**, 194–197.
7. Myers, R.H., Leavitt, J., Farrer, L.A., Jagadeesh, J., McFarlane, H., Mark, R.J. and Gusella, J.F. (1989) Homozygote for Huntington's disease. *Am. J. Hum. Genet.*, **45**, 615–618.
8. Gusella, J.F., Persichetti, F. and MacDonald, M.E. (1997) The genetic defect causing Huntington's disease: repeated in other contexts? *Mol. Med.*, **3**, 238–246.
9. Lindblad, K., Savontaus, M.L., Stevanin, G., Holmberg, M., Digre, K., Zander, C., Ehrsson, H., David, G., Benomar, A., Nikoskelainen, E. *et al.* (1996) An expanded CAG repeat sequence in spinocerebellar ataxia type 7. *Genome Res.*, **6**, 965–971.
10. Zhuchenko, O., Bailey, J., Bonnen, P., Ashizawa, T., Stockton, D.W., Amos, C., Dobyns, W.B., Subramony, S.H., Zoghbi, H.Y. and Lee, CC. (1997) Autosomal dominant cerebellar ataxia (SCA6) associated with small polyglutamine expansions in the α1A-voltage-dependent calcium channel. *Nature Genet.*, **15**, 62–68.
11. Ide, K., Nukina, N., Masuda, N., Goto, J. and Kanazawa, I. (1995) Abnormal gene product identified in Huntington's disease lymphocytes and brain. *Biochem. Biophys. Res. Commun.*, **209**, 1119–1125.
12. Trottier, Y., Lutz, Y., Stevanin, G., Imbert, G., Devys, D., Cancel, G., Saudou, F., Weber, C., David, G., Tora, L. *et al.* (1995) Polyglutamine expansion as a pathological epitope in Huntington's disease and four dominant cerebellar ataxias. *Nature*, **378**, 403–406.
13. Persichetti, F., Trettel, F., Huang, C.C., Fraefel, C., Timmers, H.T.M., Gusella, J.F. and MacDonald, M.E. (1999) Mutant huntingtin forms *in vivo* complexes with distinct context-dependent conformations of the polyglutamine segment. *Neurobiol. Dis.*, **6**, 364–375.
14. Persichetti, F., Carlee, L., Faber, P.W., McNeil, S.M., Ambrose, C.M., Srinidhi, J., Anderson, M., Barnes, G.T., Gusella, J.F. and MacDonald, M.E. (1996) Differential expression of normal and mutant Huntington's disease gene alleles. *Neurobiol. Dis.*, **3**, 183–190.
15. White, J.K., Auerbach, W., Duyao, M.P., Vonsattel, J.P., Gusella, J.F., Joyner, A.L. and MacDonald, M.E. (1997) Huntingtin is required for neurogenesis and is not impaired by the Huntington's disease CAG expansion. *Nature Genet.*, **17**, 404–410.
16. Scherzinger, E., Lurz, R., Turmaine, M., Mangiarini, L., Hollenbach, B., Hasenbank, R., Bates, G.P., Davies, S.W., Lehrach, H. and Wanker, E.E. (1997) Huntingtin-encoded polyglutamine expansions form amyloid-like protein aggregates *in vitro* and *in vivo*. *Cell*, **90**, 549–558.
17. Huang, C.C., Faber, P.W., Persichetti, F., Mittal, V., Vonsattel, J.-P., MacDonald, M.E. and Gusella, J.F. (1998) Amyloid formation by mutant huntingtin: threshold, progressivity and recruitment of normal polyglutamine proteins. *Som. Cell Mol. Genet.*, **24**, 217–233.
18. Scherzinger, E., Sittler, A., Schweiger, K., Heiser, V., Lurz, R., Hasenbank, R., Bates, G.P., Lehrach, H. and Wanker, E.E. (1999) Self-assembly of polyglutamine-containing huntingtin fragments into amyloid-like fibrils: implications for Huntington's disease pathology. *Proc. Natl Acad. Sci. USA*, **96**, 4604–4609.
19. DiFiglia, M., Sapp, E., Chase, K.O., Davies, S.W., Bates, G.P., Vonsattel, J.P. and Aronin, N. (1997) Aggregation of huntingtin in neuronal intranuclear inclusions and dystrophic neurites in brain. *Science*, **277**, 1990–1993.
20. Becher, M.W., Kotzuk, J.A., Sharp, A.H., Davies, S.W., Bates, G.P., Price, D.L. and Ross, C.A. (1998) Intranuclear neuronal inclusions in Huntington's disease and dentatorubral and pallidoluysian atrophy: correlation between the density of inclusions and IT15 CAG triplet repeat length. *Neurobiol. Dis.*, **4**, 387–397.
21. Gutekunst, C.-A., Li, S.H., Yi, H., Mulroy, J.S., Kuemmerle, S., Jones, R., Rye, D., Ferrante, R.J., Hersch, S.M. and Li, X.J. (1999) Nuclear and neuropil aggregates in Huntington's disease: relationship to neuropathology. *J. Neurosci.*, **19**, 2522–2534.
22. Maat-Schieman, M.L., Dorsman, J.C., Smoor, M.A., Siesling, S., Van Duinen, S.G., Verschuuren, J.J., den Dunnen, J.T., Van Ommen, G.J. and Roos, R.A. (1999) Distribution of inclusions in neuronal nuclei and dystrophic neurites in Huntington's disease brain. *J. Neuropath. Exp. Neurol.*, **58**, 129–137.
23. Sisodia, S.S. (1998) Nuclear inclusions in glutamine repeat disorders: are they pernicious, coincidental, or beneficial? *Cell*, **95**, 1–4.
24. Davies, S.W., Turmaine, M., Cozens, B.A., DiFiglia, M., Sharp, A.H., Ross, C.A., Scherzinger, E., Wanker, E.E., Mangiarini, L. and Bates, G.P. (1997) Formation of neuronal intranuclear inclusions (NII) underlies the neurological dysfunction in mice transgenic for the HD mutation. *Cell*, **90**, 537–548.
25. Goldberg, Y.P., Nicholson, D.W., Rasper, D.M., Kalchman, M.A., Koide, H.B., Graham, R.K., Bromm, M., Dazemi-Esfarjani, R., Thornberry, M.A., Vaillancout, J.P. and Hayden, M.R. (1996). Cleavage of huntingtin by apopain, a proapoptotic cysteine protease, is modulated by the polyglutamine tract. *Nature Genet.*, **13**, 442–449.
26. Martindale, D., Hackam, A., Wieczorek, A., Ellerby, L., Wellington, C., McCutcheon, K., Singaraja, R., Kazemi-Esfarjani, P., Devon, R., Kim, S.U. *et al.* (1998) Length of huntingtin and its polyglutamine tract influences localization and frequency of intracellular aggregates. *Nature Genet.*, **18**, 150–154.
27. Hodgson, J.G., Agopyan, N., Gutekunst, C.A., Leavitt, B.R., LePiane, F., Singaraja, R., Smith, D.J., Bissada, N., McCutcheon, K., Nasir, J. *et al.* (1999) A YAC mouse model for Huntington's disease with full-length mutant huntingtin, cytoplasmic toxicity and selective neurodegeneration. *Neuron*, **23**, 181–192.
28. Wheeler, V.C., Auerbach, W., White, J.K., Srinidhi, J., Auerbach, A., Ryan, A., Duyao, M.P., Vrbanac, V., Weaver, M., Gusella, J.F. *et al.* (1999) Length-dependent gametic CAG repeat instability in the Huntington's disease knock-in mouse. *Hum. Mol. Genet.*, **8**, 115–122.
29. Sharp, A.H. and Ross, C.A. (1996) Neurobiology of Huntington's disease. *Neurobiol. Dis.*, **3**, 3–15.
30. DiFiglia, M., Sapp, E., Chase, K., Schwarz, C., Meloni, A., Young, C., Martin, E., Vonsattel, J.P., Carraway, R., Reeves, S.A., Boyce, F.M. and Aronin N. (1995) Huntingtin is a cytoplasmic protein associated with vesicles in human and rat brain neurons. *Neuron*, **14**, 1075–1081.
31. Gutekunst, C.-A., Levey, A.I., Heilman, C.J., Whaley, W.L., Hong, Y., Nash, N.R., Rees, H.D., Madden, J.J. and Hersch, S.M. (1995) Identification and localization of huntingtin in brain and human lymphoblastoid cell lines with anti-fusion protein antibodies. *Proc. Natl Acad. Sci. USA*, **92**, 8710–8714.
32. Ferrante, R.J., Gutekunst, C.A., Persichetti, F., McNeil, S.M., Kowall, N.W., Gusella, J.F., MacDonald, M.E., Beal, M.F. and Hersch, S.M. (1997) Heterogeneous topographic and cellular distribution of huntingtin expression in the normal human neostriatum. *J. Neurosci.*, **17**, 3052–3063.
33. Ross, C.A. (1997) Intranuclear neuronal inclusions: a common pathogenic mechanism for glutamine-repeat neurodegenerative diseases? *Neuron*, **19**, 1147–1150.
34. Mangiarini, L., Sathasivam, K., Seller, M., Cozens, B., Harper, A., Hetherington, C., Lawton, M., Trottier, Y., Lehrach, H., Davies, S.W. and Bates, G.P. (1996) Exon 1 of the *HD* gene with an expanded CAG repeat is sufficient to cause a progressive neurological phenotype in transgenic mice. *Cell*, **87**, 493–506.
35. Penney, J.B., Vonsattel, J.-P., MacDonald, M.E., Gusella, J.F. and Myers, R.H. (1997) CAG repeat number governs development rate of pathology in Huntington's disease. *Ann. Neurol.*, **41**, 689–692.

36. Shelbourne, P.F., Killeen, N., Hevner, R.F., Johnston, H.M., Tecott, L., Lewandoski, M., Ennis, M., Ramirez, L., Li, Z., Iannicola, C. *et al.* (1999) A Huntington's disease CAG expansion at the murine *Hdh* locus is unstable and associated with behavioural abnormalities in mice. *Hum. Mol. Genet.*, **8**, 763–774.
37. Reddy, P.H., Williams, M., Charles, V., Garrett, L., Pike-Buchanan, L., Whetsell Jr, W.O., Miller, G. and Tagle, D.A. (1998) Behavioral abnormalities and selective neuronal loss in HD transgenic mice expressing full-length *HD* cDNA. *Nature Genet.*, **20**, 198–202.
38. Schilling, G., Becher, M.W., Sharp, A.H., Jinnah, H.A., Duan, K., Kotzuk, J.A., Slunt, H.H., Ratovitski, T., Cooper, J.K., Jenkins, N.A. *et al.* (1999) Intranuclear inclusions and neuritic aggregates in transgenic mice expressing a mutant N-terminal fragment of huntingtin. *Hum. Mol. Genet.*, **8**, 397–407 [Erratum (1999) *Hum. Mol. Genet.*, **8**, 943].
39. Gilmor, M.L., Nash, N.R., Roghani, A., Edwards, R.H., Yi, H., Hersch, S.M. and Levey, A.I. (1996) Expression of the putative vesicular acetylcholine transporter in rat brain and localization in cholinergic synaptic vesicles. *J. Neurosci.*, **16**, 2179–2190.
40. Namura, S., Zhu, J., Fink, K., Endres, M., Srinivasan, A., Tomaselli, K.J., Yuan, J. and Moskowitz, M.A. (1998) Activation and cleavage of caspase-3 in apoptosis induced by experimental cerebral ischemia. *J. Neurosci.*, **18**, 3659–3668.
41. Hurlbert, M.S., Zhou, W., Wasmeier, C., Kaddis, F.G., Hutton, J.C. and Freed, C.R. (1999) Mice transgenic for an expanded CAG repeat in the Huntington's disease gene develop diabetes. *Diabetes*, **48**, 649–651.
42. Burright, E.N., Clark, H.B., Servadio, A., Matilla, T., Feddersen, R.M., Yunis, W.S., Duvick, L.A., Zoghbi, H.Y. and Orr, H.T. (1995) SCA1 transgenic mice: a model for neurodegeneration caused by an expanded CAG trinucleotide repeat. *Cell*, **82**, 937–948.